DYNAMIC RESPONSE OF A CYLINDRICAL SHELL SEGMENT SUBJECTED TO AN ARBITRARY LOADING

NSG-571

By

Wolfram Stadler[1]

James T. S. Wang[2]

33381

ABSTRACT

Closed form expressions are obtained for the displacement, in the radial, circumferential and axial directions respectively, for a cylindrical shell segment subtended by an arbitrary angle θ_o and subjected to an arbitrary load-distribution. Laplace and finite Fourier sine and cosine transforms are employed to accomplish the solution. A numerical example, utilizing an idealized equivalent triangular blast load, is included to provide a comparison with available experimental data as found in the literature. Furthermore, the effect of the magnitude of the thickness to radius of curvature ratio $(\frac{h}{R})$, and of the negligence of the inertial terms in the axial and circumferential directions, on the frequencies, are investigated.

ACKNOWLEDGMENTS

This research was supported by NASA Research Grant No. NsG-571.

[1]Graduate Student, School of Engineering Mechanics.

[2]Associate Professor of Engineering Mechanics. Georgia Institute of Technology. Atlanta 13, Georgia 30332

INTRODUCTION

Experimental data, concerning the response of buried arches or tubes to blast wave loading is available to some extent; however, adequate theories and theoretical solutions upon which the design of such structures may be based are lacking in the literature. The present solution is to provide a step in this direction.

The investigation is restricted to the dynamic response of a simply supported cylindrical shell segment subjected to an arbitrary loading. The basic system of equations is taken directly from [5] and modified only by the inclusion of the inertia terms and forcing functions. The equations then are non-dimensionalized with respect to the length of the arch, L, the subtended angle θ_o and the decay time of the applied blast load, in order to simplify the necessary calculations. This system of linear partial differential equations is reduced to a linear algebraic system in the transformed displacement functions, by eliminating the time dependence by means of the Laplace-transformation and the spatial dependence by means of double, finite Fourier sine and cosine transforms. A simple application of Cramer's rule, and the inversion of the transformed displacement functions results in the final, closed-form solutions.

A numerical example, the dynamic response of a semicircular cylindrical shell, is included to provide a qualitative comparison to experimentally obtained data [1]. The comparison here was possible only so far as the order of magnitude is concerned, since the arch tested in [1] was stiffened considerably by the surrounding soil so that it was to be expected that the measured deflections resulting from the dynamic load would be less than those obtained by truncating the theoretical series solutions obtained in this paper. The times at which the peak deflections occurred also compare favorably.

The effect on the natural frequencies of the system, of the omission of the inertial terms in the axial and circumferential directions for varying values of the ratio $\frac{h}{R}$ is found to be negligible (of the order of 1%) for the higher frequencies, up to a certain limiting value, beyond which the inertial terms must be included.

Notation:

-	Bar above a letter denotes the Laplace transform of a function with respect to the non-dimensional time variable τ
(c)(s)	Superscripts (s) and (c) denote finite Fourier sine and cosine transforms respectively.
(cs)(cc)(ss)	Superscripts (cs), (cc) and (ss) denote successive finite Fourier transforms.
[]	Denote references in the bibliography.

Symbols:

d	Equivalent decay time.
E	Modulus of elasticity
h	Thickness of shell.
L	Length of shell.
M	Moment.
N	Normal or shear force.
p_u, p_v, p_w	Surface loading components in the directions indicated by the subscripts.
R	Radius of the cylindrical shell segment.
s	Laplacian parameter.
t	Time variable.
u,v,w	Displacements in the x,y,z-directions (Figure 1).
ν	Poisson's ratio.
ρ	Density.

Equations of Motion

The static equations of general cylindrical shell theory may be found in [5]. These equations are modified by the inclusion of the inertial forces and arbitrary forcing functions. They thence have the form:

$$\frac{\partial^2 u}{\partial x^2} + \frac{1+\nu}{2R}\frac{\partial^2 v}{\partial x \partial \theta} - \frac{\nu}{R}\frac{\partial w}{\partial x} + \frac{1-\nu}{2R^2}\frac{\partial^2 u}{\partial \theta^2} = -\frac{(1-\nu^2)}{Eh}\left(p_u - \rho h \frac{\partial^2 u}{\partial t^2}\right)$$

$$\frac{1+\nu}{2R}\frac{\partial^2 u}{\partial x \partial \theta} + \frac{1-\nu}{2}\frac{\partial^2 v}{\partial x^2} + \frac{\partial^2 v}{R^2 \partial \theta^2} - \frac{\partial w}{R^2 \partial \theta} = -\frac{(1-\nu^2)}{Eh}\left(p_v - \rho h \frac{\partial^2 v}{\partial t^2}\right) \qquad (1)$$

$$\nu \frac{\partial u}{\partial x} + \frac{1}{R}\frac{\partial v}{\partial \theta} - \frac{w}{R} - \frac{h^2 R}{12}\left(\frac{\partial^4 w}{\partial x^4} + \frac{2}{R^2}\frac{\partial^4 w}{\partial x^2 \partial \theta^2} + \frac{1}{R^4}\frac{\partial^4 w}{\partial \theta^4}\right) = \frac{-R(1-\nu^2)}{Eh}\left(p_w - \rho h \frac{\partial^2 w}{\partial t^2}\right)$$

where the loading components p_u, p_v, and p_w are functions of x, θ, and t.

The problem is completely formulated, when the following boundary and initial conditions are included:

a) initial conditions:

$$w(x,\theta,0) = u(x,\theta,0) = v(x,\theta,0) = 0;$$

$$w_t(x,\theta,0) = u_t(x,\theta,0) = v_t(x,\theta,0) = 0;$$

b) boundary conditions:

i) imposed on θ

$$\begin{aligned} u(x,0,t) &= u(x,\theta_o,t) = 0; \\ v_\theta(x,0,t) &= v_\theta(x,\theta_o,t) = 0; \\ w(x,0,t) &= w(x,\theta_o,t) = 0; \\ w_{\theta\theta}(x,0,t) &= w_{\theta\theta}(x,\theta_o,t) = 0; \end{aligned} \qquad (2)$$

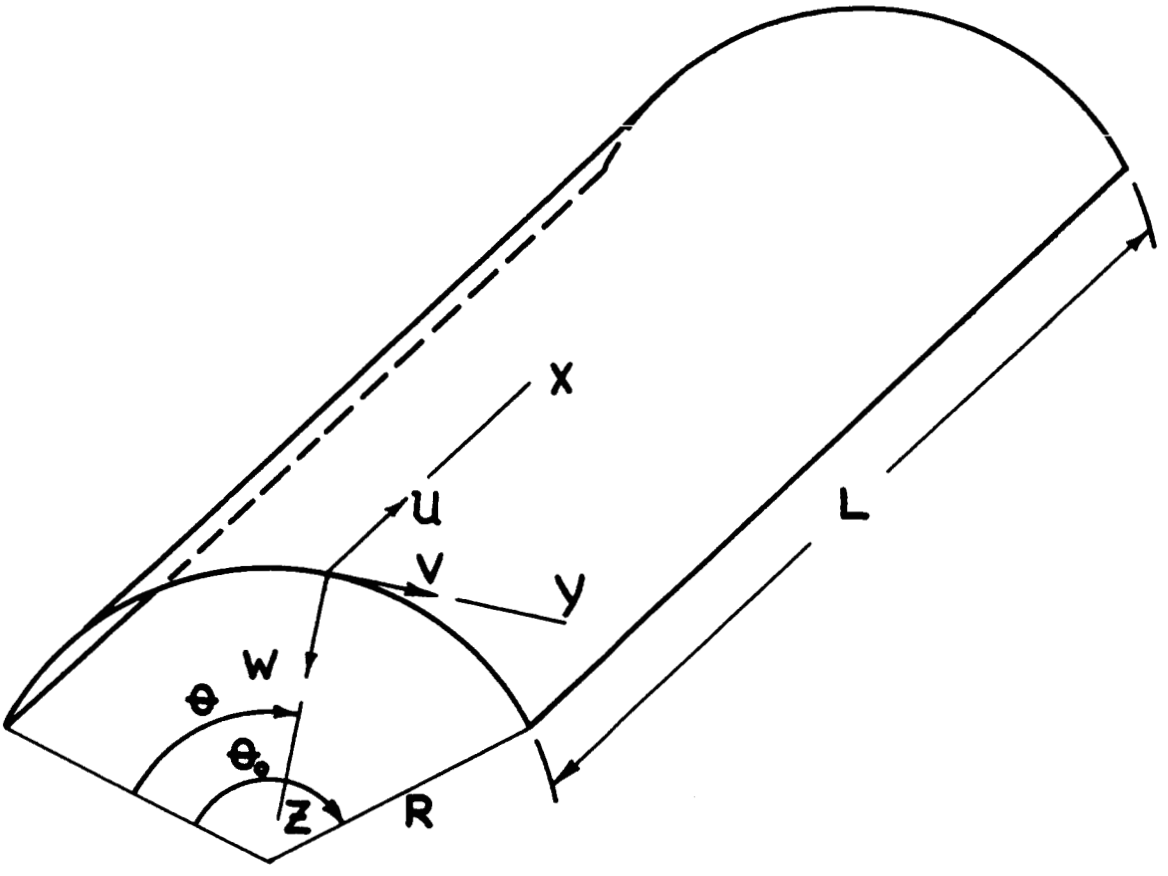

FIG. 1
CYLINDRICAL SHELL SEGMENT

ii) imposed on x

$$u_x(0,\theta,t) = u_x(L,\theta,t) = 0;$$
$$v(0,\theta,t) = v(L,\theta,t) = 0;$$
$$w(0,\theta,t) = w(L,\theta,t) = 0;$$
$$w_{xx}(0,\theta,t) = w_{xx}(L,\theta,t) = 0,$$

where the subscript notation has been used to denote partial differentiation.

It is convenient to non-dimensionalize equations (1), and (2), by introducing the following non-dimensional ratios:

$$\xi = \frac{x}{L};\ \varphi = \frac{\theta}{\theta_o};\ \tau = \frac{t}{d};\ U = \frac{u}{L};\ V = \frac{v}{L};\ W = \frac{w}{L};\ p_u^* = \frac{p_u}{E};\ p_v^* = \frac{p_v}{E};\ p_w^* = \frac{p_w}{E},$$

where d is the equivalent decay time of the shock-load. This characteristic constant is used since the prime concern here is blast and impulsive loading. The substitution of these non-dimensional variables in equation (1) and the subsequent Laplace transformation of these equations, in conjunction with the initial conditions results in

$$\frac{\partial^2\bar{U}}{\partial\xi^2} + a_1\frac{\partial^2\bar{V}}{\partial\xi\partial\varphi} - a_2\frac{\partial\bar{W}}{\partial\xi} + a_3\frac{\partial^2\bar{U}}{\partial\varphi^2} = -a_4\bar{p}_u^* + a_5 s^2\bar{U} \qquad (a)$$

$$\frac{\partial^2\bar{V}}{\partial\xi^2} + b_1\frac{\partial^2\bar{U}}{\partial\xi\partial\varphi} - b_2\frac{\partial\bar{W}}{\partial\varphi} + b_3\frac{\partial^2\bar{V}}{\partial\varphi^2} = -b_4\bar{p}_v^* + b_5 s^2\bar{V} \qquad (b) \qquad (3)$$

$$\frac{\partial\bar{U}}{\partial\xi} + c_1\frac{\partial\bar{V}}{\partial\varphi} - c_2\bar{W} - c_3\frac{\partial^4\bar{W}}{\partial\xi^4} - c_4\frac{\partial^4\bar{W}}{\partial\xi^2\partial\varphi^2} - c_5\frac{\partial^4\bar{W}}{\partial\varphi^4} \qquad (c)$$

$$= -c_6\bar{p}_w^* + c_7 s^2\bar{W}$$

where

$$a_1 = \frac{L}{\theta_o}\frac{1+\nu}{2R} \qquad b_1 = \frac{L(1+\nu)}{R\theta_o(1-\nu)} \qquad c_1 = \frac{L}{\nu R\theta_o} \qquad c_6 = \frac{R(1-\nu^2)}{h\nu}$$

$$a_2 = \frac{\nu L}{R} \qquad b_2 = \frac{2L^2}{R^2\theta_o(1-\nu)} \qquad c_2 = \frac{L}{\nu R} \qquad c_7 = \frac{R(1-\nu^2)\rho L}{E\nu d^2}$$

$$a_3 = \frac{L^2(1-\nu)}{2R^2\theta_o^2} \qquad b_3 = \frac{2L^2}{R^2\theta_o^2(1-\nu)} \qquad c_3 = \frac{h^2R}{12L^3\nu}$$

$$a_4 = \frac{L(1-\nu^2)}{h} \qquad b_4 = \frac{2L(1+\nu)}{h} \qquad c_4 = \frac{h^2}{6RL\nu\theta_o^2}$$

$$a_5 = \frac{(1-\nu^2)\rho L^2}{Ed^2} \qquad b_5 = \frac{2(1+\nu)L^2\rho}{Ed^2} \qquad c_5 = \frac{h^2L}{12\nu R^3\theta_o^4}$$

and where it is assumed that the p's are Laplace-transformable.

The linear system (3) of partial differential equations is now transformed to a linear system of algebraic equations by the application of finite Fourier sine and cosine transforms [4](see also appendix), with the boundary conditions (2), i.e.

$$\begin{aligned}
&(A_{11} + s^2)\,\bar{U}^{(cs)}(m,n,s) + A_{12}\bar{V}^{(sc)}(m,n,s) + A_{13}\bar{W}^{(ss)}(m,n,s) = \bar{Q}_1(m,n,s)\\
&A_{21}\bar{U}^{(cs)}(m,n,s) + (A_{22} + s^2)\bar{V}^{(sc)}(m,n,s) + A_{23}\bar{W}^{(ss)}(m,n,s) = \bar{Q}_2(m,n,s)\\
&A_{31}\bar{U}^{(cs)}(m,n,s) + A_{32}\bar{V}^{(sc)}(m,n,s) + (A_{33} + s^2)\bar{W}^{(ss)}(m,n,s) = \bar{Q}_3(m,n,s).
\end{aligned} \tag{4}$$

Here, the superscripts indicate the type of transformation and the order in which they were carried out. Furthermore, the arguments (m,n,s) of the transformed functions are order-preserving with respect to the arguments (ξ,φ,τ) of the original functions. The coefficients A_{ij} in equation (4) are given by

$$A_{11} = \frac{\alpha_m^2 + a_3\beta_n^2}{a_5};\quad A_{12} = \frac{a_1\alpha_m\beta_n}{a_5};\quad A_{13} = -\frac{a_2\alpha_m}{a_5};\quad \bar{Q}_1 = \frac{a_4}{a_5}\,\bar{\bar{p}}_u^{*(cs)};$$

$$A_{21} = \frac{\alpha_m\beta_n b_1}{b_5};\quad A_{22} = \frac{\alpha_m^2 + b_3\beta_n^2}{b_5};\quad A_{23} = \frac{b_2\beta_n}{b_5};\quad \bar{Q}_2 = \frac{b_4}{b_5}\,\bar{\bar{p}}_v^{*(sc)}; \tag{5}$$

$$A_{31} = \frac{\alpha_m}{c_7};\quad A_{32} = \frac{c_1\beta_n}{c_7};\quad A_{33} = \frac{c_2 + c_3\alpha_m^4 + c_4\alpha_m^2\beta_n^2 + c_5\beta_n^4}{c_7};\quad \bar{Q}_3 = \frac{c_6}{c_7}\,\bar{\bar{p}}_w^{*(ss)},$$

where $\alpha_m = \pi m$ and $\beta_n = \pi n$ are the transform parameters for ξ and φ respectively.

An investigation of these coefficients A_{ij} reveals that they are symmetric, which was to be expected from the symmetry of the original equations. This symmetry becomes quite useful if one observes that the s^2's may be interpreted as the eigenvalues of a real, symmetric matrix, obtained from equation (4), and as such must be real [2]. With this in mind, Cramer's rule may be applied to equation (4) and the solutions written in the form:

$$\bar{U}^{(cs)}(m,n,s) = \sum_{j=1}^{3} \bar{Q}_j\,\bar{K}_{1j}(m,n,s)$$

$$\bar{V}^{(sc)}(m,n,s) = \sum_{j=1}^{3} \bar{Q}_j\,\bar{K}_{2j}(m,n,s) \tag{6}$$

$$\bar{W}^{(ss)}(m,n,s) = \sum_{j=1}^{3} \bar{Q}_j\,\bar{K}_{3j}(m,n,s)$$

where the $\bar{Q}_j$'s are the loading functions as defined in (5) and where

$$\bar{K}_{ij}(m,n,s) = \frac{C_{ij}}{s^2+\omega_1^2} + \frac{D_{ij}}{s^2+\omega_2^2} + \frac{E_{ij}}{s^2+\omega_3^2} \tag{7}$$

with

$$C_{11} = \frac{(\omega_2^2-\omega_3^2)[\omega_1^4-(A_{22}+A_{33})\omega_1^2+A_{22}A_{33}-A_{23}^2]}{\Delta(\omega^2)}$$

$$C_{12} = C_{21} = \frac{(\omega_2^2-\omega_3^2)[A_{12}\omega_1^2+A_{13}A_{23}-A_{12}A_{33}]}{\Delta(\omega^2)}$$

$$C_{13} = C_{31} = \frac{(\omega_2^2-\omega_3^2)[A_{13}\omega_1^2+A_{12}A_{23}-A_{13}A_{22}]}{\Delta(\omega^2)}$$

$$C_{22} = \frac{(\omega_2^2-\omega_3^2)[\omega_1^4-(A_{11}+A_{33})\omega_1^2+A_{11}A_{33}-A_{13}^2]}{\Delta(\omega^2)}$$

$$C_{23} = \frac{(\omega_2^2-\omega_3^2)[A_{23}\omega_1^2+A_{12}A_{13}-A_{11}A_{23}]}{\Delta(\omega^2)}$$

$$C_{33} = \frac{(\omega_2^2-\omega_3^2)[\omega_1^4-(A_{11}+A_{22})\omega_1^2+A_{11}A_{22}-A_{12}^2]}{\Delta(\omega^2)}$$

$$D_{11} = \frac{(\omega_3^2-\omega_1^2)[\omega_2^4-(A_{22}+A_{33})\omega_2^2+A_{22}A_{33}-A_{23}^2]}{\Delta(\omega^2)}$$

$$D_{12} = D_{21} = \frac{(\omega_3^2-\omega_1^2)(A_{12}\omega_2^2+A_{13}A_{23}-A_{12}A_{33})}{\Delta(\omega^2)}$$

$$D_{13} = D_{31} = \frac{(\omega_3^2-\omega_1^2)(A_{13}\omega_2^2+A_{12}A_{23}-A_{13}A_{22})}{\Delta(\omega^2)}$$

$$D_{22} = \frac{(\omega_3^2-\omega_1^2)[\omega_2^4-(A_{11}+A_{33})\omega_2^2+A_{11}A_{33}-A_{13}^2]}{\Delta(\omega^2)}$$

$$D_{23} = D_{32} = \frac{(\omega_3^2-\omega_1^2)\ [A_{23}\omega_2^2+A_{12}A_{13}-A_{11}A_{23}]}{\Delta(\omega^2)}$$

$$D_{33} = \frac{(\omega_3^2-\omega_1^2)[\omega_2^4-(A_{11}+A_{22})\omega_2^2+A_{11}A_{22}-A_{12}^2]}{\Delta(\omega^2)}$$

$$E_{11} = \frac{(\omega_1^2-\omega_2^2)[\omega_3^4-(A_{22}+A_{33})\omega_3^2+A_{22}A_{33}-A_{23}^2]}{\Delta(\omega^2)}$$

$$E_{12} = E_{21} = \frac{(\omega_1^2-\omega_2^2)[\ A_{12}\omega_3^2+A_{13}A_{23}-A_{12}A_{33}]}{\Delta(\omega^2)}$$

$$E_{13} = E_{31} = \frac{(\omega_1^2-\omega_2^2)[\ A_{13}\omega_3^2+A_{12}A_{23}-A_{13}A_{22}]}{\Delta(\omega^2)}$$

$$E_{22} = \frac{(\omega_1^2-\omega_2^2)[\omega_3^4-(A_{11}+A_{33})\omega_3^2+A_{11}A_{33}-A_{13}^2]}{\Delta(\omega^2)}$$

$$E_{23} = E_{32} = \frac{(\omega_1^2-\omega_2^2)[\ A_{23}\omega_3^2+A_{12}A_{13}-A_{11}A_{23}]}{\Delta(\omega^2)}$$

$$E_{33} = \frac{(\omega_1^2-\omega_2^2)[\omega_3^4-(A_{11}+A_{22})\omega_3^2+A_{11}A_{22}-A_{12}^2]}{\Delta(\omega^2)}$$

and

$$\Delta(\omega^2) = (\omega_1^2 - \omega_2^2)(\omega_1^2 - \omega_3^2)(\omega_2^2 - \omega_3^2)$$

as obtained by some algebraic manipulation and by means of a partial fractions separation.

The ω_i's are obtained by setting $s^2 = -\lambda_i$ in the determinant of the coefficient matrix of equations (4), and then solving the cubic equation

$$\lambda^3 + \theta_1\lambda^2 + \theta_2\lambda + \theta_3 = 0 \tag{9}$$

obtained by expansion of the determinant. Here, θ_1, θ_2 and θ_3 are given by

$$\theta_1 = (A_{11}+A_{22}+A_{33})$$

$$\theta_2 = (A_{11}A_{22}+A_{11}A_{33}+A_{22}A_{33}-A_{12}^2-A_{13}^2-A_{23}^2)$$

$$\theta_3 = (A_{11}A_{22}A_{33}+2A_{12}A_{13}A_{23}-A_{12}^2A_{33}-A_{13}^2A_{22}-A_{23}^2A_{11})$$

From Descartes' rule for the roots of a polynominal it is known that (9) can have only negative roots as long as $\theta_1, \theta_2, \theta_3 > 0$. Since this must be the case, if the solution is to remain stable, it is justifiable to write the solution in the form (6).

The inversion of equations (6) with respect to the Laplace transformation is now accomplished through the application of the convolution integral defined by

$$L^{-1}\{f(s)g(s)\} = F(\tau)*G(\tau) = \int_0^\tau F(\tau-t)G(t)dt$$

The result is

$$U^{(cs)}(m,n,\tau) = \sum_{j=1}^{3} \int_{o}^{\tau} Q_j(m,n,\zeta) K_{1j}(m,n,\tau-\zeta)\,d\zeta$$

$$V^{(sc)}(m,n,\tau) = \sum_{j=1}^{3} \int_{o}^{\tau} Q_j(m,n,\zeta) K_{2j}(m,n,\tau-\zeta)\,d\zeta \qquad (10)$$

$$W^{(ss)}(m,n,\tau) = \sum_{j=1}^{3} \int_{o}^{\tau} Q_j(m,n,\zeta) K_{3j}(m,n,\tau-\zeta)\,d\zeta$$

where

$$Q_1(m,n,\zeta) = kp_u^{*(cs)}(m,n,\zeta)$$

$$Q_2(m,n,\zeta) = kp_v^{*(cs)}(m,n,\zeta)$$

$$Q_3(m,n,\zeta) = kp_w^{*(ss)}(m,n,\zeta)$$

since

$$\frac{a_4}{a_5} = \frac{b_4}{b_5} = \frac{c_6}{c_7} = \frac{Ed^2}{\rho h L} = k.$$

Also,

$$L^{-1}\left\{\bar{K}_{ij}(m,n,s)\right\} = K_{ij}(m,n,\tau)$$

$$= \frac{C_{ij}}{\omega_1} \sin \omega_1\tau + \frac{D_{ij}}{\omega_2} \sin \omega_2\tau + \frac{E_{ij}}{\omega_3} \sin \omega_3\tau,$$

$L^{-1}\{\ \}$ denoting the inverse Laplace transform.

The final step in obtaining the solution of the system of equations (1) is the inversion of the Fourier sine and cosine transforms. These operations are carried out with the use of the inverse transforms as defined in the

appendix. The inversion may be separated into two parts:

a) inversion w.r.t. φ

$$U^{(c)}(m,\varphi,\tau) = 2\sum_{n=1}^{\infty}\left\{\sum_{j=1}^{3}\int_{o}^{\tau} Q_j(m,n,\zeta)K_{1j}(m,n,\tau-\zeta)d\zeta\right\}\sin\beta_n\varphi$$

$$V^{(s)}(m,\varphi,\tau) = V^{(sc)}(m,0,\tau) + 2\sum_{n=1}^{\infty}\left\{\sum_{j=1}^{3}\int_{o}^{\tau} Q_j(m,n,\zeta)K_{2j}(m,n,\tau-\zeta)d\zeta\right\}\cos\beta_n\varphi$$

$$W^{(s)}(m,\varphi,\tau) = 2\sum_{n=1}^{\infty}\left\{\sum_{j=1}^{3}\int_{o}^{\tau} Q_j(m,n,\zeta)K_{3j}(m,n,\tau-\zeta)d\zeta\right\}\sin\beta_n\varphi \qquad (11)$$

b) inversion w.r.t. ξ

$$U(\xi,\varphi,\tau) = U^{(c)}(0,\varphi,\tau) + 4\sum_{m=1}^{\infty}\sum_{n=1}^{\infty}\left\{\sum_{j=1}^{3}\int_{o}^{\tau} Q_j(m,n,\zeta)K_{1j}(m,n,\tau-\zeta)d\zeta\right\}$$

$$\sin\beta_n\varphi\cos\alpha_m\xi$$

$$V(\xi,\varphi,\tau) = 2\sum_{m=1}^{\infty}\left\{V^{(sc)}(m,0,\tau) + 2\sum_{n=1}^{\infty}\left\{\sum_{j=1}^{3}\int_{o}^{\tau} Q_j(m,n,\zeta)K_{2j}(m,n,\tau-\zeta)d\zeta\right\}\cos\beta_n\varphi\right\}$$

$$\sin\alpha_m\xi \qquad (12)$$

$$W(\xi,\varphi,\tau) = 4\sum_{m=1}^{\infty}\sum_{n=1}^{\infty}\left\{\sum_{j=1}^{3}\int_{o}^{\tau} Q_j(m,n,\zeta)K_{3j}(m,n,\tau-\zeta)d\zeta\right\}\sin\beta_n\varphi\sin\alpha_m\xi$$

Equations (12) represent the solution of the dynamic equations of a cylindrical shell segment subjected to an arbitrary loading, arbitrary to the extent, naturally, that the loading function be Fourier transformable.

The expressions for the stresses and moments in terms of the displacements are given by [5]

$$
\begin{aligned}
N_{xx} &= N\left[\frac{\partial u}{\partial x} + \frac{\nu}{R}\left(\frac{\partial v}{\partial \theta} - w\right)\right];\\
N_{\theta\theta} &= N\left[\frac{1}{R}\left(\frac{\partial v}{\partial \theta} - w\right) + \nu\frac{\partial u}{\partial x}\right];\\
N_{x\theta} &= \frac{1}{2}N(1-\nu)\left[\frac{1}{R}\frac{\partial u}{\partial \theta} + \frac{\partial v}{\partial x}\right];\\
M_{xx} &= -D\left[\frac{\partial^2 w}{\partial x^2} + \frac{\nu}{R^2}\left(\frac{\partial v}{\partial \theta} + \frac{\partial^2 w}{\partial \theta^2}\right)\right];\\
M_{\theta\theta} &= -D\left[\frac{1}{R^2}\left(\frac{\partial v}{\partial \theta} + \frac{\partial^2 w}{\partial \theta^2}\right) + \nu\frac{\partial^2 w}{\partial x^2}\right];\\
M_{x\theta} &= D(1-\nu)\frac{1}{R}\left[\frac{\partial v}{\partial x} + \frac{\partial^2 w}{\partial x \partial \theta}\right].
\end{aligned}
\tag{13}
$$

where $N = \frac{Eh}{1-\nu^2}$ and $D = \frac{Eh^3}{12(1-\nu^2)}$. Note that equations (13) are in terms of the dimensional variables.

Comparison with Experimental Data

Unfortunately, no experimental data are available which correspond exactly to simple support conditions. Of the considered experimental data, that which most closely approximates the case of simply supported edges is obtained from [1], where a buried arch subjected to short and long duration blast-loading is considered. In order to keep the numerical calculations as simple as possible, this type of loading is simulated by an equivalent (equivalent in the sense of the same total impulse) triangular pulse load of the form

$$p_w = p_o \left(1 - \frac{t}{d}\right),$$

where p_o represents the peak overpressure, and d is the equivalent decay time. Transformation and substitution in equation (12) results in

$$w(\xi,\varphi,\tau) = \frac{4p_o d^2}{h\rho L\pi^2} \sum_{m=1}^{\infty} \sum_{n=1}^{\infty} [1-(-1)^m-(-1)^n+(-1)^{m+n}].$$

$$\left\{\frac{C_{33}}{\omega_1^2} [1-\tau-\cos\omega_1\tau+\frac{1}{\omega_1}\sin\omega_1\tau] + \frac{D_{33}}{\omega_2^2} [1-\tau-\cos\omega_2\tau+\frac{1}{\omega_2}\sin\omega_2\tau] + \frac{E_{33}}{\omega_3^2} [1-\tau-\cos\omega_3\tau+\frac{1}{\omega_3}\sin\omega_3\tau]\right\}$$

$$\sin \alpha_m\xi \sin \beta_n\varphi. \qquad (14)$$

This expression, with the particular values:

$$h = .0478 \text{ in}, \quad L = 57.6 \text{ in}, \quad \rho = 1.3564 \times 10^{-3} \frac{\text{lb sec}^2}{\text{in}^4},$$

$$p_o = 7.5 \text{ psi}, \quad d = 76 \text{ msec}, \quad E = 30 \times 10^6 \text{ psi}, \quad \theta_o = \pi$$

is used to obtain the deflections in non-dimensional form.

The experimental and theoretical data can be compared only in order of magnitude due to the discrepancies mentioned above. In the numerical evaluation of equation (12), care must be exercised in truncating the resultant

series, since convergence is slow. The difficulty arises for fixed m, with n increasing, since the radial frequency, ω_1, initially decreases, and thereafter monotonically increases for some n depending on m. The

TABLE 1

Numerical Comparison with Experimental Data

	Experimental	Theoretical
$\bar{\omega}_1 \left(\begin{smallmatrix} m=1 \\ n=3 \end{smallmatrix}\right) \frac{cyd}{msec}$	.105	.132
Peak Crown Deflection in inches	.172	.535
Max. Response at Crown in msec	15	36

interval, in which ω_1 decreases, becomes smaller with a decrease in θ_o, i.e. approaching the shallow shell range, and with an increase in $\frac{h}{R}$. From Figure 2 it is apparent that, in view of the large difference in frequencies the omission of the inertial terms for u and v has little effect for the lower modes. Figure 3 indicates that there is a peak deflection at 13 msec. This, however, is a relative maximum; the maximum occurs at 36 msec as indicated in Table 1. The difference in the numerical values of the deflections is explained in [1] as the result of a difference in soil density, i.e. small reductions in soil density resulted in a large percentage increase in the deflection. The frequency in Table 1, corresponding to the first inextensional symmetrical mode, was measured with no endwalls in the arch. Since simple supports were assumed in the numerical example, an increase in the frequency is to be expected. The absence, in the theoretical response curve (Figure 3), of the damping exhibited for the experimental deflection curve is to be attributed to the rough approximation given by the triangular load.

Effect of the Omission of the Inertial Terms in the Axial and Circumferential Directions.

The investigation of the omission of the inertial terms is restricted to the effect on the radial frequency. The effect on the deflection is not considered. The frequencies, as obtained here, are compared to those calculated from the expression [4]

$$\omega_1^* = \frac{1}{h\rho R^2}\left[\frac{N}{R^2}(\lambda^2_m + \mu^2_n)^2 + \frac{Eh\lambda^4_m}{(\lambda^2_m+\mu^2_n)^2}\right] \qquad (15)$$

where

$$N = \frac{Eh^3}{12(1-\nu^2)};\ \lambda_m = \frac{m\pi R}{L};\ \mu_n = \frac{n\pi}{\theta_o}.$$

Equation (15) is based on shallow shell theory, omitting the inertial terms in the u and v -directions. For the higher frequencies there is virtually no error introduced by using (15), even out of shallow shell range. However, the error in the fundamental frequency (m=1, n=1) increases as θ_o increases, and becomes 41% for $\theta_o=\pi$. The frequencies increase with increasing $\frac{h}{R}$ up to $\frac{h}{R} = \frac{1}{20}$, which was taken to be the upper bound for thin shell theory [3]. Again, the error introduced by using (15) instead of (9) to obtain the frequencies is negligible.

It must be emphasized that the range of applicability of equation (15) is limited to a certain frequency range. As was discovered by E. Reissner [6] for spherical shells, there also exist limiting values of the frequencies of a cylindrical shell segment, beyond which, the inertial terms must be included. It was not yet possible to determine an indicative parameter. The range of applicability of (15) decreases as $\frac{h}{R}$ increases and as θ_o decreases. As can be seen from Table 2, equation (15) is useless for $\frac{h}{R} = \frac{1}{20}$ when $n \geq 15$, $m = 1$, or for $\frac{h}{R} = \frac{1}{45}$ when $n \geq 31$, $m = 1$. (The latter values do not appear in the table).

TABLE 2

NON-DIMENSIONAL FREQUENCIES
(m = 1)

	$\theta_o = \pi$		$\theta_o = \frac{\pi}{3}$									
$\frac{h}{R}$	$\frac{1}{300}$		$\frac{1}{300}$		$\frac{1}{200}$		$\frac{1}{100}$		$\frac{1}{45}$		$\frac{1}{20}$	
h	ω_1	ω_1^*	ω_1	ω_1^*	ω_1	ω_1^*	ω_1	ω_1^*	ω_1	ω_1^*	ω_1	ω_1^*
1	214.5	302.1	47.1	49.7	47.9	50.5	51.6	54.4	67.8	71.5	120.37	126.97
3	49.7	52.6	63.2	63.5	98.8	99.5	197.5	198.6	438.3	440.9	987.0	992.9
5	26.5	27.1	174.5	174.9	273.9	274.4	547.7	548.8	1215.9	1218.4	2738.2	2744.3
7	37.1	37.5	342.0	342.3	536.6	537.2	1073.1	1074.3	2382.3	2384.9	5365.2	5371.5
9	59.3	59.7	565.2	565.6	886.9	887.5	1773.7	1774.9	3937.6	3940.2	8867.7	8874.5
11	88.1	88.5	844.3	844.6	1324.7	1325.3	2649.4	2650.6	5881.7	5884.4	13245	13253
13	122.9	123.3	1179.1	1179.5	1850.1	1850.1	3700.3	3701.5	8214.6	8217.4	18498	18507
15	163.6	164.0	1570.0	1570.2	2463.2	2463.7	4926.4	4927.5	10936.0	10939.0	21723	24637
17	210.1	210.5	2016.4	2016.7	3163.8	3164.3	6327.5	6328.7	14047.0	14049.0	24619	31643
19	262.5	262.8	2518.7	2519.0	3952.0	3952.1	7904.0	7905.1	17546.0	17549.0	27514	39525

Conclusions

The response of a cylindrical shell segment, subtended by an arbitrary angle θ_o and subjected to an arbitrary loading, is obtained, based on thin shell theory.

In summary:

1. Inertial terms affect mainly the frequency corresponding to the first inextensional mode in the radial direction. (n = 1, m increasing).
2. The introduced error increases with decreasing $\frac{h}{R}$.
3. To obtain the frequencies corresponding to the higher longitudinal modes ($n \geq 15$ for $\frac{h}{R} = \frac{1}{20}$ and m = 1) the inertial terms must be included.
4. Comparisons with experimental data are favorable as far as order of magnitude is concerned.

APPENDIX

The Fourier sine and cosine transforms are given by [4]:

a) Single transforms:

Sine transform: $f^{(s)}(n) = \int_0^a f(\varphi)\sin\beta_n\varphi d\varphi.$

Cosine transform: $f^{(c)}(n) = \int_0^a f(\varphi)\cos\beta_n\varphi d\varphi.$

Single inverse transforms:

Inverse sine transform: $f(\varphi) = \frac{2}{a}\sum_{n=1}^{\infty} f^{(s)}(n)\sin\beta_n\varphi.$

Inverse cosine transform: $f(\varphi) = \frac{1}{a}f^{(c)}(0) + \frac{2}{a}\sum_{n=1}^{\infty} f^{(c)}(n)\cos\beta_n\varphi.$

b) Simple double transforms:

Double sine transform: $f^{(ss)}(m,n) = \int_0^b\int_0^a f(\xi,\varphi)\sin\alpha_m\xi\sin\beta_n\varphi d\varphi d\xi.$

Double cosine transform: $f^{(cc)}(m,n) = \int_0^b\int_0^a f(\xi,\varphi)\cos\alpha_m\xi\cos\beta_n\varphi d\varphi d\xi.$

Inverse simple double transforms:

Inverse double sine transform: $f(\xi,\varphi) = \frac{4}{ab}\sum_{n=1}^{\infty}\sum_{m=1}^{\infty} f^{(ss)}(m,n)\sin\alpha_m\xi\sin\beta_n\varphi.$

Inverse double cosine transform:

$$f(\xi,\varphi) = \frac{1}{a^2}f^{(cc)}(0,0) + \frac{2}{a^2}\sum_{n=1}^{\infty} f^{(cc)}(0,n)\cos\beta_n\varphi + \frac{2}{a^2}\sum_{m=1}^{\infty}\left\{f^{(cc)}(m,0)+2\sum_{n=1}^{\infty} f^{(cc)}(m,n)\cos\alpha_m\xi\right\}\cos\beta_n\varphi.$$

c) Mixed double transforms:

Sine-cosine transform: $$f^{(sc)}(m,n) = \int_0^b \int_0^a f(\xi,\varphi)\sin\alpha_m\xi\cos\beta_n\varphi d\varphi d\xi$$

Cosine-sine transform: $$f^{(cs)}(m,n) = \int_0^b \int_0^a f(\xi,\varphi)\cos\alpha_m\xi\sin\beta_n\varphi d\varphi d\xi$$

Inverse mixed double transforms:

Inverse sine-cosine transform: $$f(\xi,\varphi) = \frac{2}{a^2}\sum_{m=1}^{\infty}\left\{f^{(sc)}(m,0) + 2\sum_{n=1}^{\infty} f^{(sc)}(m,n)\cos\beta_n\varphi\right\}\sin\alpha_m\xi$$

Inverse cosine-sine transform: $$f(\xi,\varphi) = \frac{2}{a^2}\sum_{n=1}^{\infty} f^{(cs)}(0,n)\sin\beta_n\varphi + \frac{4}{a^2}\sum_{m=1}^{\infty}\sum_{n=1}^{\infty} f^{(cs)}(m,n)\sin\beta_n\varphi\cos\alpha_m\xi$$

where $\alpha_m = \frac{m\pi}{b}$ and $\beta_n = \frac{n\pi}{a}$.

Note that, in general

$$f^{(sc)}(m,n) \neq f^{(cs)}(m,n)$$

It is clear that when these transform methods are applied the relevant assumptions concerning the functions to be transformed are made, namely that they satisfy Dirichlet's conditions in their respective intervals, and that the iterated integrals may be taken successively, i.e.

$$f^{(s)}(m,\varphi) = \int_0^b f(\xi,\varphi)\sin\alpha_m\xi\, d\xi$$

and

$$f^{(sc)}(m,n) = \int_0^a f^{(s)}(m,\varphi)\cos\beta_n\varphi d\varphi.$$

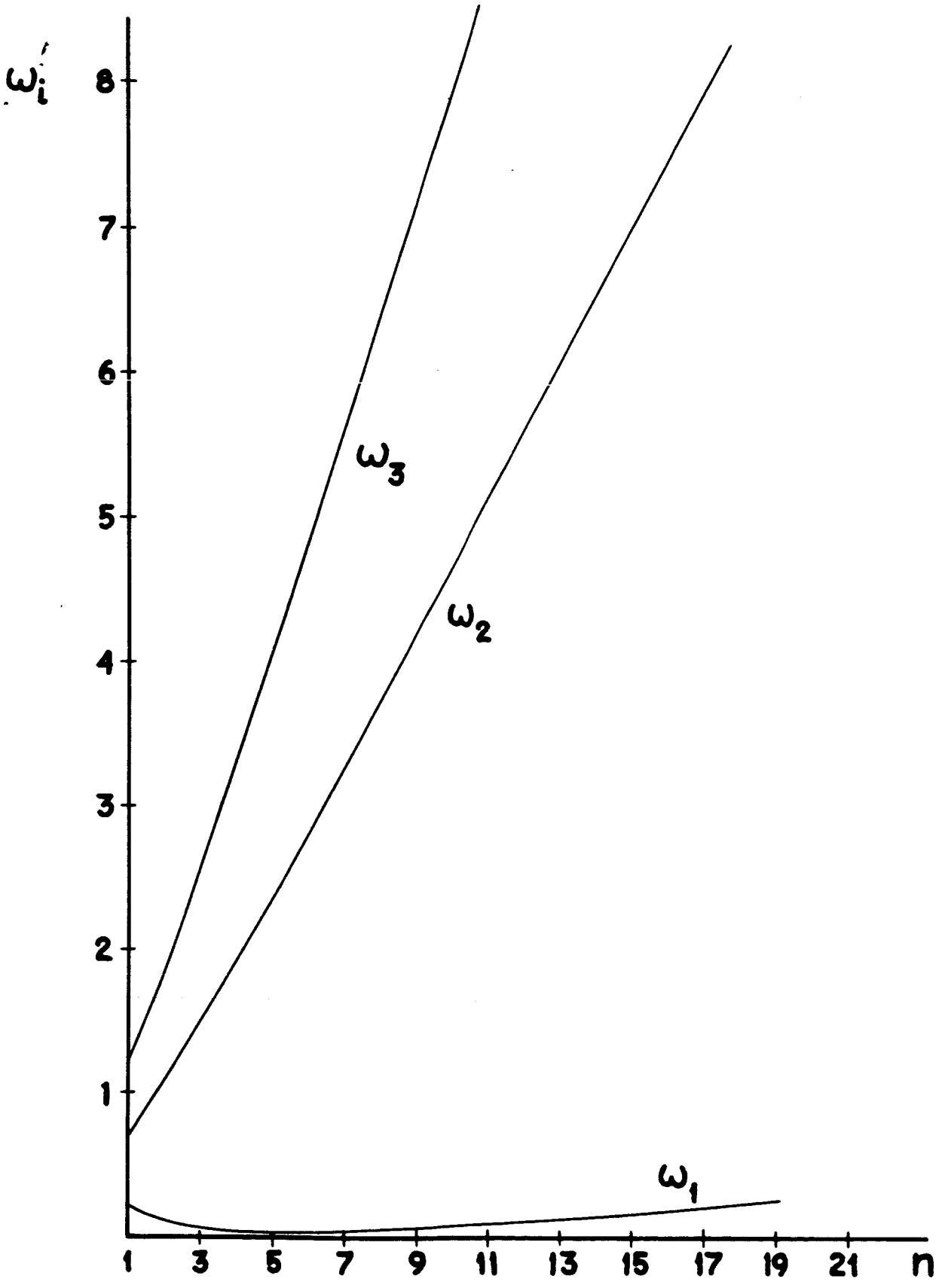

FIG. 2
NONDIM. FUNDAMENTAL FREQUENCIES

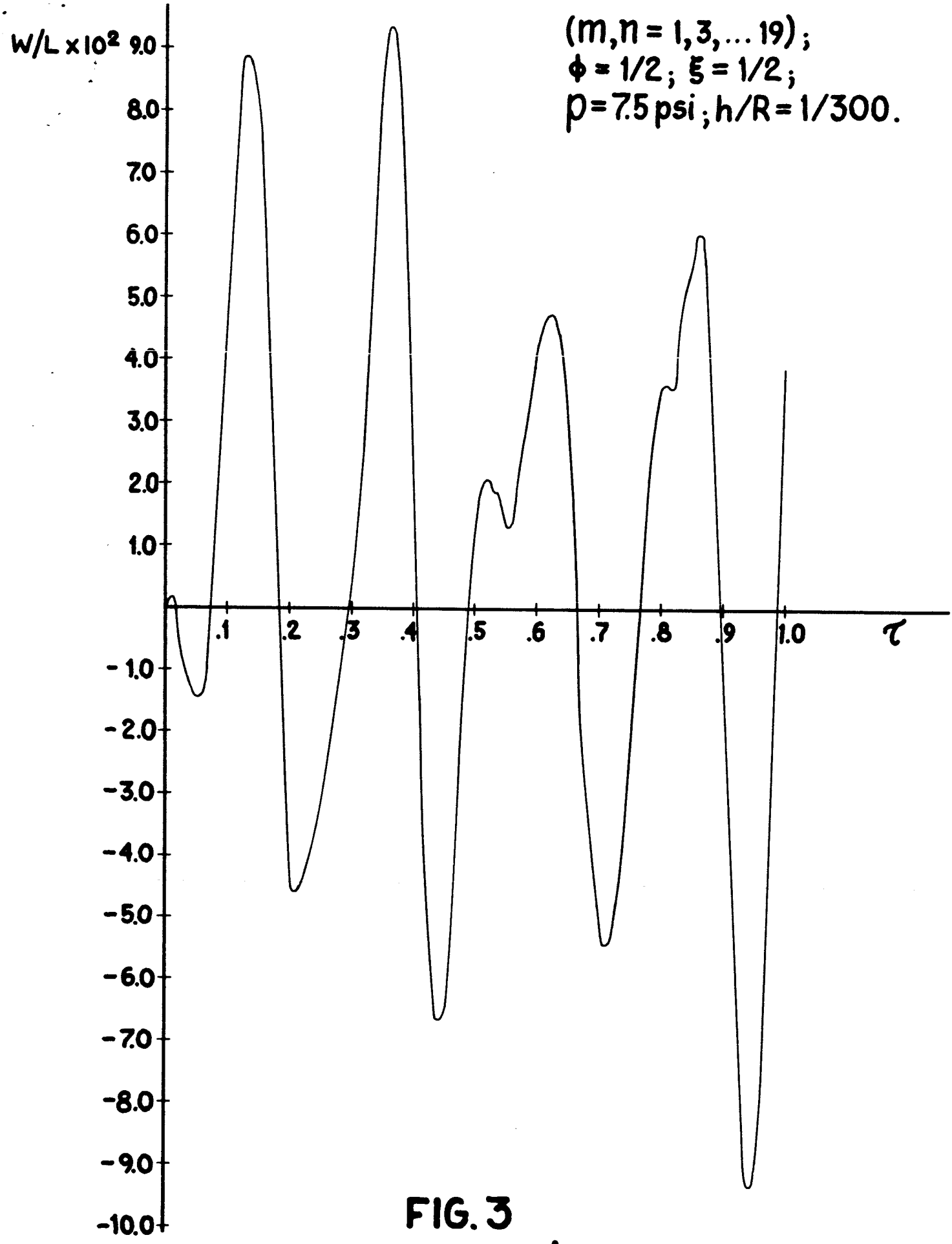

FIG. 3
W/L VS τ

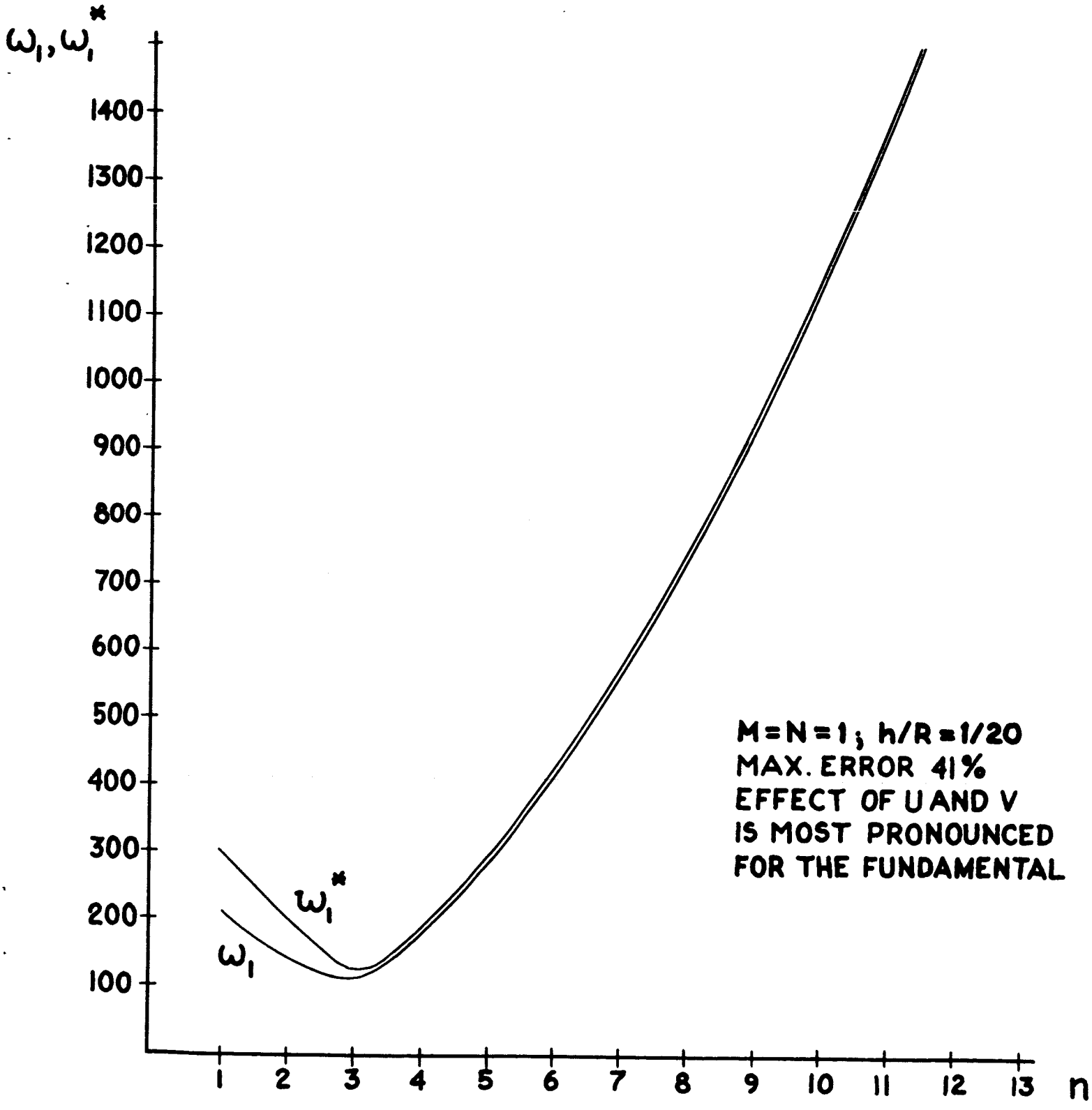

FIG. 4
ω_1, ω_1^* VS n

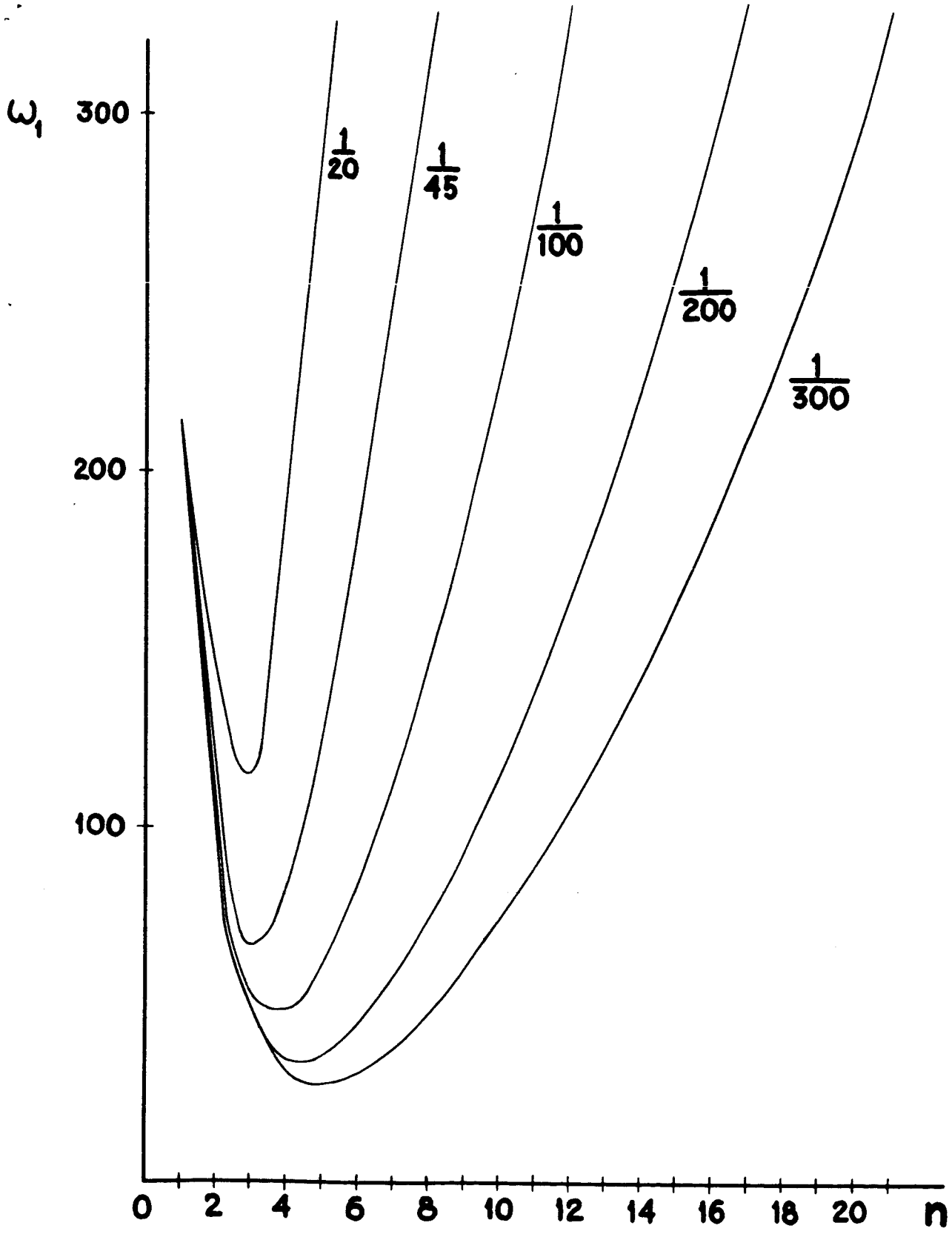

FIG. 5

ω_1 VS n FOR VARYING h/R

BIBLIOGRAPHY

1. Jay R. Allgood, "Blast Loading of Small Buried Arches," Journal of the Structural Division, Proceedings of the American Society of Civil Engineers, vol. 90, No. St5, 1964, pp. 39-61.

2. F. B. Hildebrand. Methods of Applied Mathematics. Prentice Hall, 1961.

3. V. V. Novoshilov. Theory of Thin Shells. Ove Arup and Partners, London, 1959.

4. W. Nowacki. Dynamics of Elastic Systems. John Wiley and Sons, Inc., New York, 1963, p. 267.

5. S. Timoshenko, S. Woinowsky-Krieger. Theory of Plates and Shells. McGraw-Hill, New York, 1959, p. 514, p. 432.

6. E. Reissner, "On Transverse Vibrations of Thin, Shallow Elastic Shells," Quarterly of Applied Mathematics 13, pp. 169-176, 1955.

Dynamic Response of a Cylindrical Shell Segment Subjected to an Arbitrary Loading.

List of errata

1. page 1 - 3rd to last line, "Graduate Research Assistant" instead of "Graduate Student"

2. page 12 - Immediately following the definitions of θ_1, θ_2 and θ_3 Descartes' instead of Descarte's

3. page 12 - Two lines below 2.) - justifiable instead of justifyable

4. page 12 - Last equation on the page; the variable of integration should be

   ζ instead of t

5. page 13 - Last equation on the page;

   ζ instead of τ

6. page 15 - Last sentence

   "are stated in terms of" instead of "are in terms of"

7. page 16 - Last paragraph, first sentence should be,. . . .discrepancies mentioned above, and the fact that the calculated values for the deflections are out of the small deflection range. In the . . . .

8. page 17 - In table 1,

   $\bar{\omega}_1$ instead of ω_1

   $\frac{\text{cycl}}{\text{m sec}}$ instead of $\frac{\text{cyd}}{\text{m sec}}$

9. page 18 - The denominator of the second term of equation (15) should be

   $(\lambda^2_m + \mu^2_n)^2$ instead of $(\lambda^2_m + \mu_n^2)$

10. page 20 - Rewrite p. 20, as follows:

Conclusions

The response of a cylindrical shell segment, subtended by an arbitrary angle θ_o and subjected to an arbitrary loading, is obtained, based on thin shell theory.

In summary:

A. Comparison of the exact frequencies with those obtained from shallow shell theory.

   1. Inertial terms affect mainly the radial frequency corresponding to the first circumferential mode (n = 1; m increasing).

   2. The error in the frequencies introduced by neglecting inertial terms, is virtually unaffected by changes in $\frac{h}{R}$ for a given θ_o.

3. The error in the frequencies introduced by neglecting inertial terms, increases for increasing θ_o. It is noteworthy that only the modes corresponding to n = 1, 2, 3 are affected; for the higher modes the frequencies obtained by means of the shallow shell theory differ only slightly from the exact frequencies. Hence expression (15) may be used to calculate frequencies for shell segments out of shallow shell range.

4. To obtain the frequencies corresponding to the higher circumferential modes (e.g. $n \geq 15$ for $\frac{h}{R} = \frac{1}{20}$ and m = 1) the inertial terms must be included.

B. Comparison of the theoretical results with experimental data.

1. Times, at which peak deflections occur, subsequent to loading, agree well with those obtained experimentally.

2. Maximum deflections compare favorably with experimental values, as far as order of magnitude is concerned. The discrepancies may be ascribed to the stiffening effect of the sand-loading of the arch, and to the fact that the calculated theoretical values are somewhat out of the small deflection range, (small in comparison to the thickness).

3. The theoretical and experimental frequencies, corresponding to the first inextensional symmetrical mode, were in good agreement. Unfortunately no further experimentally obtained frequencies were available.